UNSTEADY SIMULATION OF ICED SWEPT WINGS USING ANISOTROPIC SUBGRID MODE BASED IDDES METHOD

Ziyu Zhou¹, Maochao Xiao² Dian Li³ and Yufei Zhang^{1†}

¹ School of Aerospace Engineering, Tsinghua University, Beijing 100084, China

² Department of mechanical and aerospace engineering, Sapienza University of Rome, Rome 00184, Italy

³ AVIC Xi'an Aeronautics Computing Technique Research Institute, Shaanxi 710000, China

zhouziyu23@mails.tsinghua.edu.cn – maochao.xiao@uniroma1.it – dian.li@hotmail.com –
zhangyufei@tsinghua.edu.cn

† Corresponding Author

Abstract

This paper presents the AMD-IDDES method, an improved Delayed Detached Eddy Simulation (IDDES) approach incorporating an anisotropic minimum dissipation (AMD) model, to simulate unsteady flow over an iced swept-wing. Results show that AMD-IDDES predicts K-H instability and small-scale vortices more accurately, improves flow velocity diffusion in the wingtip separation zone, and provides more precise reattachment locations and pressure recovery, outperforming the standard IDDES method.

1. Introduction

When an aircraft passes through an icing cloud, the aircraft surface is impacted by a large number of supercooled water droplets, leading to the occurrence of icing. Icing disrupts the original aerodynamic shape of the aircraft, causing premature boundary layer transition and early flow separation[1,2]. Typical effects of icing include increased drag, reduced stall angle of attack, and decreased maximum lift. In recent years, aviation safety incidents caused by icing have frequently occurred both domestically and internationally. In 2006, a KJ-200 early warning aircraft crashed due to wing icing; in 2016, a Boeing 737-800 passenger aircraft in Dubai crashed due to wing icing; and in 2021, a Beidahuang General Aviation B-10GD aircraft became unstable and crashed due to severe wing icing[3]. Aircraft icing has long posed a serious threat to aviation safety.

Since 1997, the U.S. National Transportation Safety Board (NTSB) has identified icing as one of the most critical factors affecting aviation safety. Numerous organizations, including the NTSB, the Commercial Aviation Safety Team (CAST), the Federal Aviation Administration (FAA), and the National Aeronautics and Space Administration (NASA), have invested substantial resources in icing research tunnel (IRT) experiments and computational fluid dynamics (CFD) studies to improve understanding of the icing process and the aerodynamic effects of icing. These efforts have led to significant progress in designing anti-icing systems, improving certification procedures, and enhancing pilot training, thereby reducing risks associated with icing[4].

Research on icing problems primarily focuses on two aspects: the icing process and aerodynamic characteristics. Research on the icing process aims to explore the mechanisms of icing, analyze the process of supercooled water droplets freezing into ice, and determine the critical ice shape to provide a foundation for subsequent aerodynamic studies. Research on aerodynamic characteristics aims to analyze the flow around fixed ice shapes and ensure that aircraft can maintain reliability and safety under harsh conditions such as critical ice shapes. This is a key step in aircraft airworthiness certification and safety assessment.

This study investigates the aerodynamic effects of icing on swept wings using unsteady simulation methods based on fixed ice shapes. The complexity of separated flow over iced airfoils places high demands on the accuracy of turbulence modeling methods [4]. However, China's current research on aircraft icing still has many shortcomings, particularly the lack of high-accuracy computational tools for predicting the aerodynamic characteristics of iced wings. Therefore, developing high-accuracy turbulence models suitable for predicting separated flow over iced wings is essential.

2. Computational methodology

2.1 IDDES

The IDDES approach based on two-equation SST $k-\omega$ model[5] is formulated by substituting the RANS length scale with the IDDES length scale in the destruction term of the turbulent kinetic energy (TKE) transport equation while keeping the ω equation unmodified. The TKE equation of the SST-IDDES can be written as[6]

$$\frac{\partial(\rho k)}{\partial t} + \frac{\partial(\rho u_j k)}{\partial x_j} = P_k - \frac{\rho k^{\frac{3}{2}}}{l_{IDDES}} + \frac{\partial}{\partial x_j} \left[(\mu + \sigma_k \mu_t) \frac{\partial k}{\partial x_j} \right]$$
(1)

where k is the modeled TKE. The IDDES length scale l_{IDDES} is defined as

$$l_{\text{IDDES}} = f_d (1 + f_e) l_{\text{RANS}} + (1 - f_d) l_{\text{LES}}$$
 (2)

where $l_{RANS} = \sqrt{k}/C_{\mu}\omega$ and $l_{LES} = C_{DES}\Delta$ are the turbulent length scale of the RANS and the subgrid length scale of the LES. The length scale Δ in l_{LES} of simplified IDDES model[7] is defined as $\Delta = \min\{C_w \max[d_w, \Delta_{max}], \Delta_{max}\}$. The shielding function f_d and an elevating function f_e are added in Eq. (2) to control the switch between RANS and LES branches and to increase the eddy viscosity in the RANS region before the RANS/LES switch, respectively.

2.2 AMD-IDDES

Rozema [8] proposed a anisotropic minimum dissipation (AMD) model, which provided the minimum eddy current dissipation required to remove sub filter scale energy from the LES solution. An unique advantage of the AMD model is its good performance on anisotropic grids, as demonstrated by Haering [9] in the decaying isotropic turbulence case. This model locally approximates exact dissipation and is consistent with the nonlinear gradient model, providing the necessary scale separation for eddy viscosity. For simplicity, it is assumed that the filter box Ω_{δ} is rectangular with dimensions Δx , Δy , and Δz . For ease of formula expression, these dimensions can also be written as Δ_k . The eddy viscosity of the AMD model is

$$\nu_t = C_A^2 \frac{-\Delta_k^2 g_{ik} g_{jk} S_{ij}}{g_{ml} g_{ml}} \tag{4}$$

where $\delta x_i \partial_i$ is the scaled gradient operator, $S_{ij} = (\partial_i v_j + \partial_j v_i)/2$ is the resolved rate-of-strain tensor, $g_{ij} = \partial u_i/\partial x_j$ and C_A is a consistent. Zhou et al.[10] combined the AMD subgrid model with the IDDES method to propose the AMD-IDDES method. This method aims to leverage the advantages of the AMD model in anisotropic grids to improve the accuracy of simulations using the IDDES method. The LES length scale in the AMD-IDDES method can be obtained as:

$$l_{LES} = C_{A} \left(\frac{\gamma}{\beta}\right)^{\frac{3}{4}} \left(\frac{-\Delta_{k}^{2} g_{ik} g_{jk} S_{ij}}{g_{ml} g_{ml} S}\right)^{\frac{1}{2}}$$

$$(5)$$

This can also be written as

$$l_{LES} = C_{DES,AMD} \Delta_{AMD} \tag{6}$$

$$C_{DES,AMD} = C_{A} \left(\frac{\gamma}{\beta}\right)^{\frac{3}{4}}, \Delta_{AMD} = \left(\frac{-\Delta_{k}^{2} g_{ik} g_{jk} S_{ij}}{g_{ml} g_{ml} S}\right)^{\frac{1}{2}}$$

$$(7)$$

where, $C_{DES,AMD}$ is set to be 2.40 in the program.

2.3 Other Numerical Methods

The Navier-Stokes equations are solved using the in-house structured finite volume solver NSAWE[11]. The inviscid flux is discretized via a hybrid central/upwind scheme; the central part is a fourth-order central difference scheme, and the upwind part is a fifth-order Roe/WENO scheme. The viscous flux is approximated via a second-order central

difference scheme. Time advancement is performed by an implicit dual-time-step lower-upper symmetric Gauss-Seidel (LU-SGS) scheme.

3. Computational Setup

As shown in the experimental data from references [12–14], the model is a 30-degree swept wing with a chord length of 17.32 inches and a span of 35.18 inches. The airfoil section (in the plane perpendicular to the leading edge) is NACA 0012. The icing model used is a simulated ice accumulation based on measurements of ice accretion on a NACA 0012 airfoil in NASA icing research. The icing conditions include a freestream velocity of 80.782km/h, an angle of attack of 4 degrees, an icing duration of 5 minutes, droplets with a volume median diameter of $20\mu m$, $LWC = 2.1g/m^3$, and a temperature of 265.37K. Under these conditions, the resulting ice formation is horn ice (clear ice) with prominent protruding structures. The computational model is shown in Figure 1.

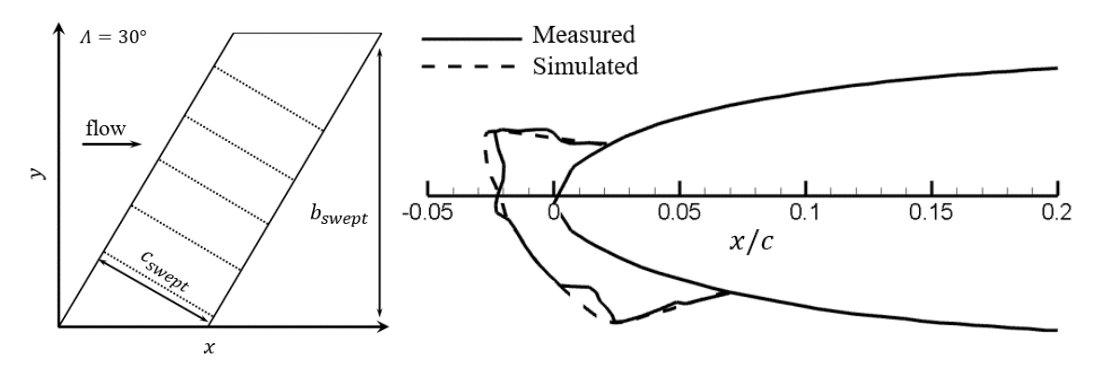


Figure 1: Computational model

The computational case used in this chapter is for Ma = 0.2, $Re = 1.2 \times 10^6$ and $AOA = 8^\circ$. The computational domain and boundary conditions are the same as those in reference [12], with a streamwise length of 3.3 m, a spanwise width of 1.22 m, and a height of 0.92 m. The computational grid is shown in Figure 2, with a total grid count of approximately 53 million. The inlet total pressure is $P_t/P_\infty = 1.02828$, the total temperature is $T_t/T_\infty = 1.008$, and the outlet is set as a static pressure boundary with $P/P_\infty = 1.0$. A symmetry boundary condition is applied at the root-side boundary upstream of the wing, while adiabatic no-slip wall conditions are applied to the other surfaces. The tip-side boundary is also treated as an adiabatic no-slip wall. The dimensionless time step for the computation is $\Delta t U_\infty/c = 0.001$, with 40 inner iteration steps.

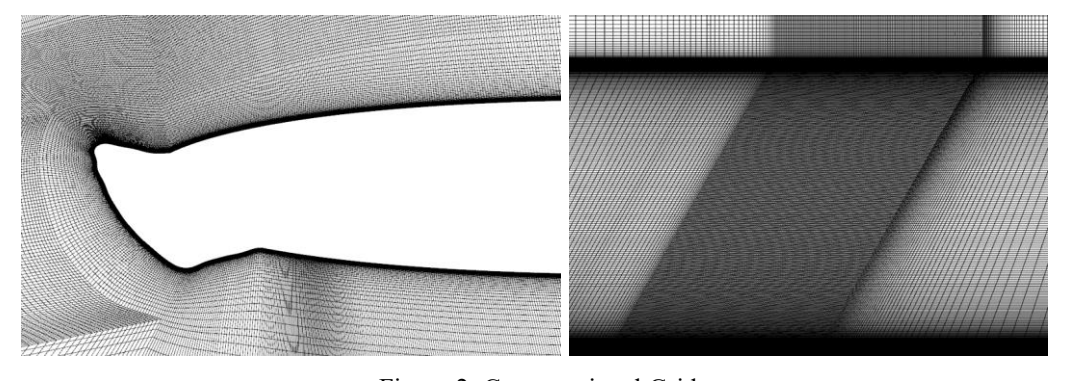


Figure 2: Computational Grid

4. Computational Results

4.1 Instantaneous result

Figure 3 compares the instantaneous vortex structures obtained using the standard IDDES and AMD-IDDES methods. It can be observed that at the leading edge of the wing, icing causes a strong reverse pressure after the wing leading edge, leading to flow separation behind the ice and the detachment of the free shear layer at the top of the ice formation. The free shear layer becomes unstable downstream through K-H instability, generating two-dimensional vortex

structures, which gradually evolve into three-dimensional structures as they propagate downstream, with an increase in vortex scale. Additionally, due to the presence of sweep angle, a leading-edge vortex first forms at the root of the wing and then develops towards the wingtip, where larger-scale vortex structures are formed. The spanwise flow associated with these vortex structures is particularly evident. Further comparison between the standard IDDES and AMD-IDDES methods reveals that, at the wing leading edge and mid-span, the AMD-IDDES method is able to simulate the K-H instability phenomenon earlier and resolve smaller-scale vortices.

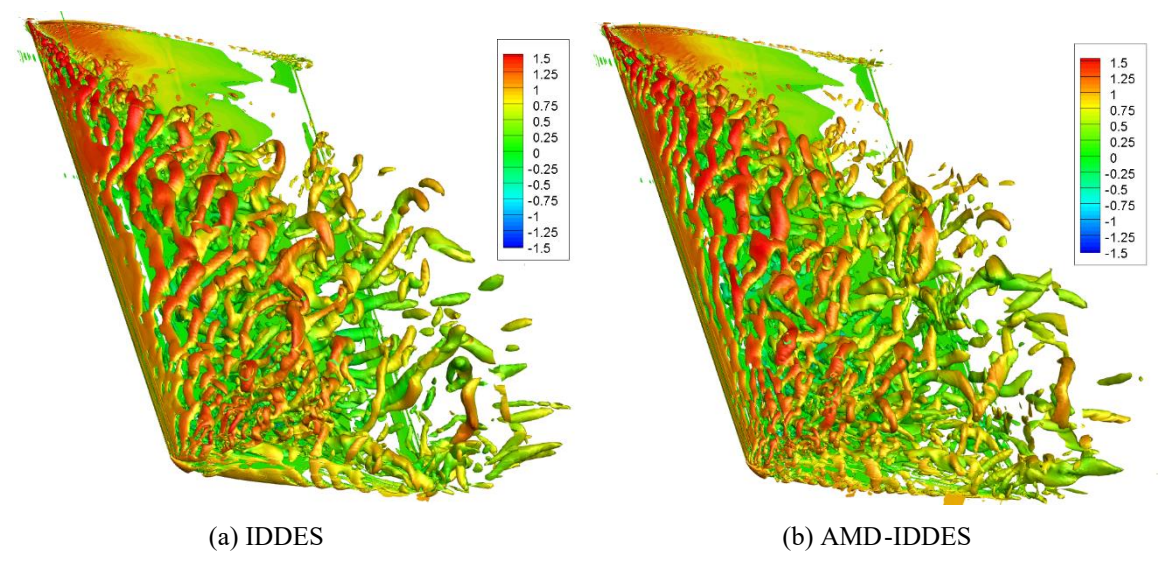


Figure 3: Instantaneous vortex structures $(Q(c/U_{\infty})^2 = 40.0$, colored by streamwise velocity u_x/U_{∞})

Figure 4 and Figure 5 present the instantaneous streamwise velocity distribution at different spanwise positions, with the specific locations shown in Figure 1. The free shear layer behind the leading-edge ice undergoes K-H instability downstream, generating vortex structures that promote the mixing of low-energy fluid in the separation zone with high-energy fluid in the mainstream. This results in the formation of a separation bubble at the leading edge of the wing, and as the spanwise position increases, the length of the separation bubble grows. Comparing the results obtained from the standard IDDES and AMD-IDDES methods, it is observed that the streamwise velocity in the standard IDDES method diffuses more slowly, with the simulated low-speed separation region being longer than that predicted by the AMD-IDDES method. Additionally, near the wingtip, the simulated low-speed separation region is located farther downstream, leading to excessive drag and a downward pitching moment at the nose of the wing.

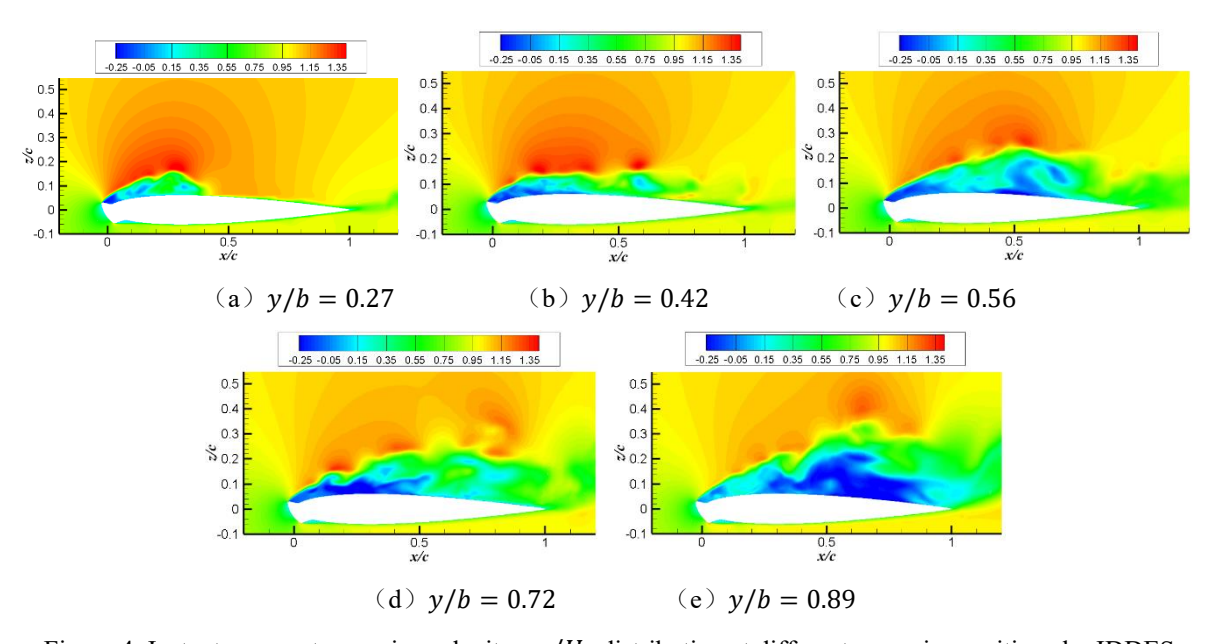


Figure 4: Instantaneous streamwise velocity u_x/U_∞ distribution at different spanwise positions by IDDES

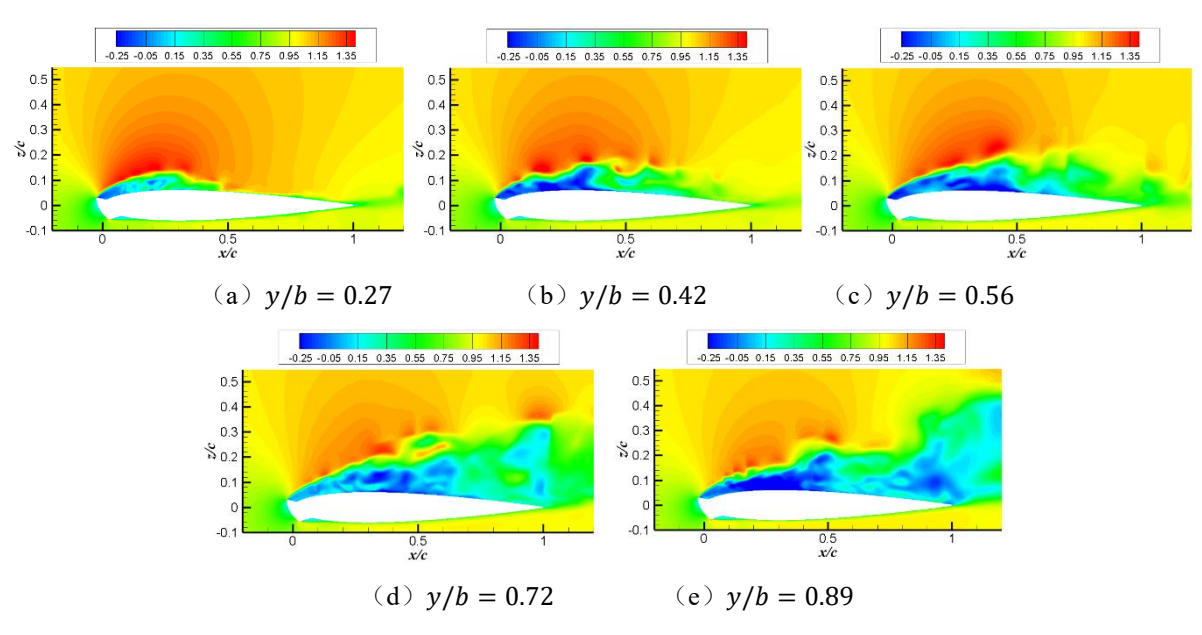


Figure 5: Instantaneous streamwise velocity u_x/U_∞ distribution at different spanwise positions by AMD-IDDES

Figure 6 and Figure 7, along with Figure 8 and. Figure 9, show the distribution of instantaneous eddy viscosity and vorticity at different spanwise positions. Comparing the results obtained from the standard IDDES and AMD-IDDES methods, it can be observed that in the shear layer separation region, the standard IDDES method results in larger eddy viscosity, and the formation of the leading-edge vortex occurs later. In contrast, the AMD-IDDES method effectively reduces the eddy viscosity in the shear separation region, alleviating the "gray area issue."

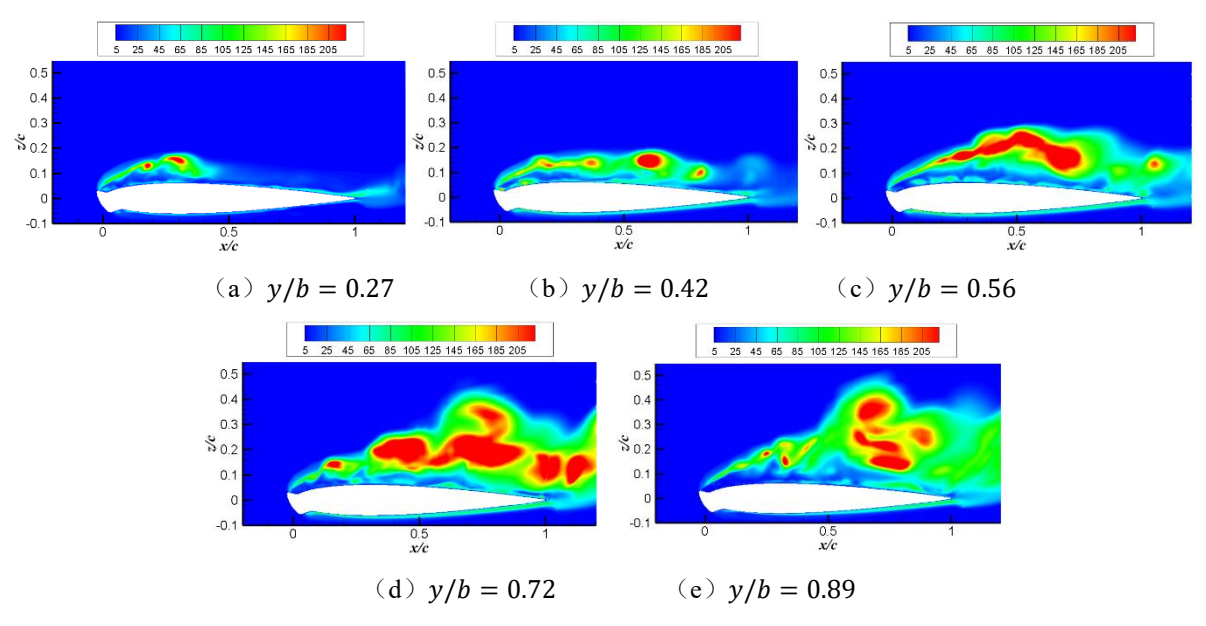
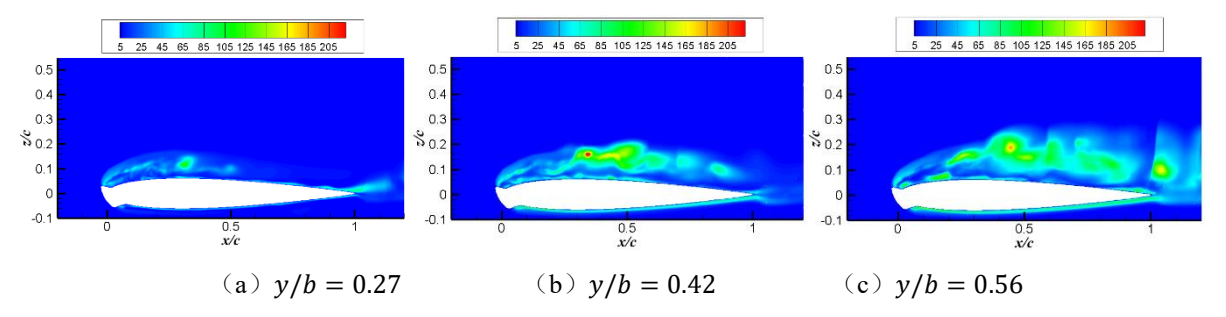


Figure 6: Instantaneous eddy viscosity μ_t/μ distribution at different spanwise positions by IDDES



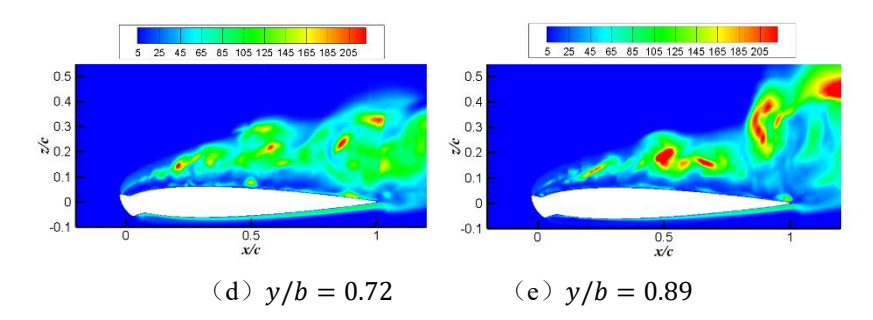


Figure 7: Instantaneous eddy viscosity μ_t/μ distribution at different spanwise positions by AMD-IDDES

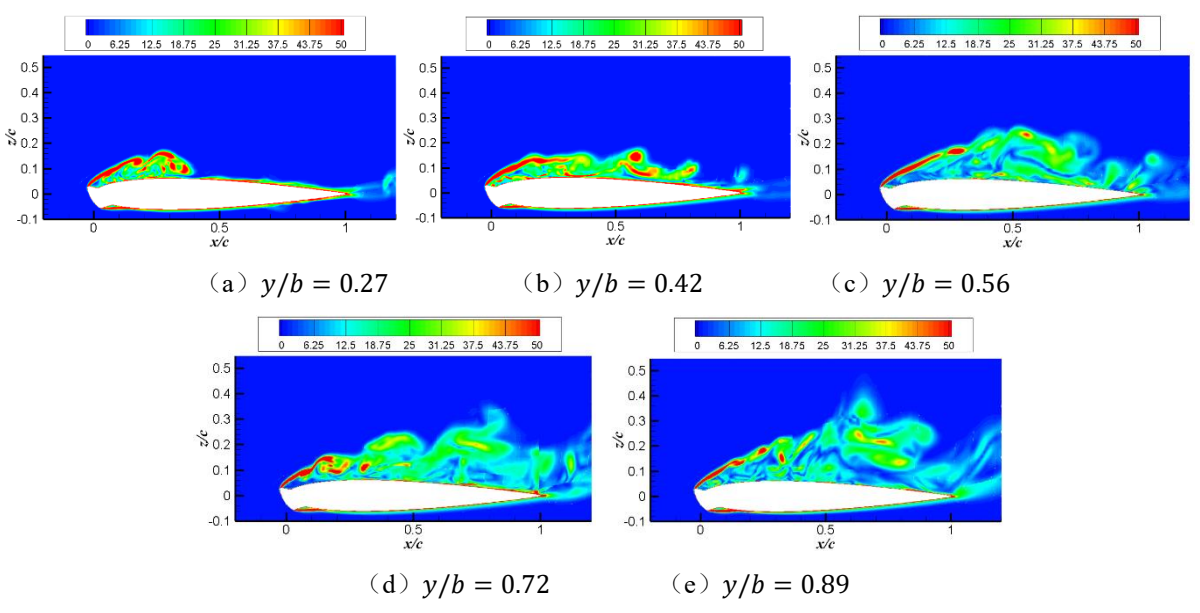


Figure 8: Instantaneous vorticity $\Omega c/U_{\infty}$ distribution at different spanwise positions by IDDES

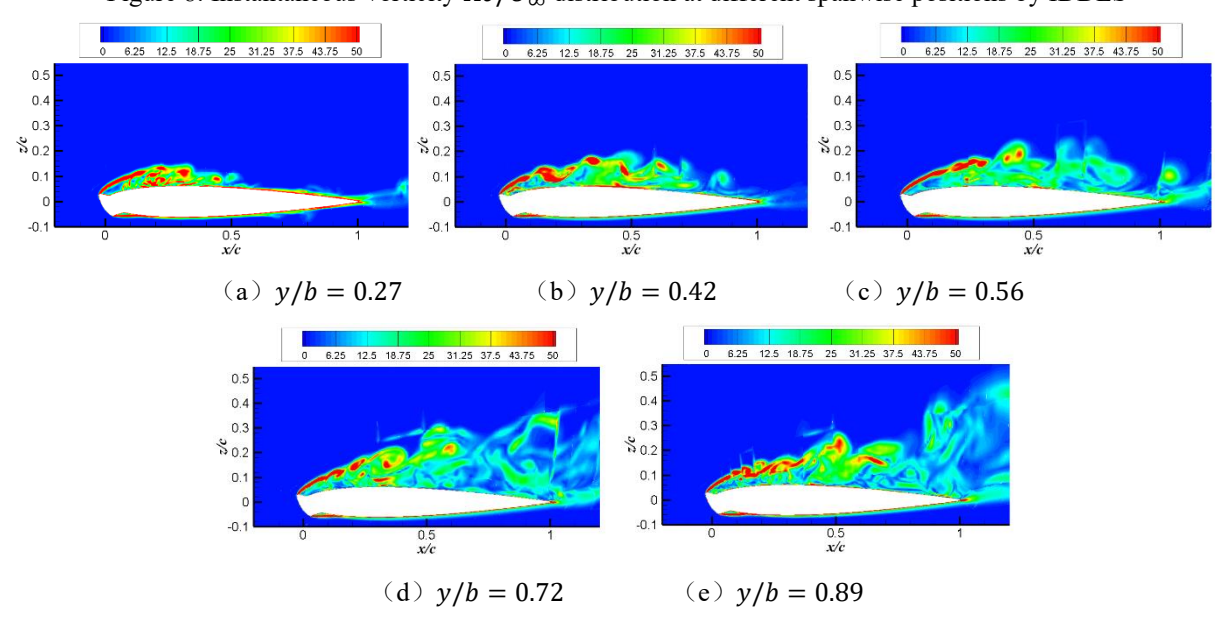


Figure 9: Instantaneous vorticity $\Omega c/U_{\infty}$ distribution at different spanwise positions by AMD-IDDES

4.2 Average result

Figure 10 shows the pressure distribution at different spanwise positions simulated by the RANS, standard IDDES, and AMD-IDDES methods, compared with experimental results for the clean wing and iced wing. The pressure

distribution indicates that leading-edge icing causes the suction peak at the wing's leading edge to be replaced by a nearly constant pressure plateau, which covers about 20-40% of the chord length. This suggests the presence of a leading-edge separation bubble in the flow field. Downstream of the pressure plateau is the pressure recovery region, where, after a certain level of pressure recovery, turbulence in the shear layer reattaches downstream under the influence of pressure. This behavior is similar to the surface pressure distribution found in laminar separation bubbles[15]. In fact, in the pressure plateau region, the pressure shows a gradual decline, which is due to the reverse velocity reaching its maximum value just beneath the recirculation zone.

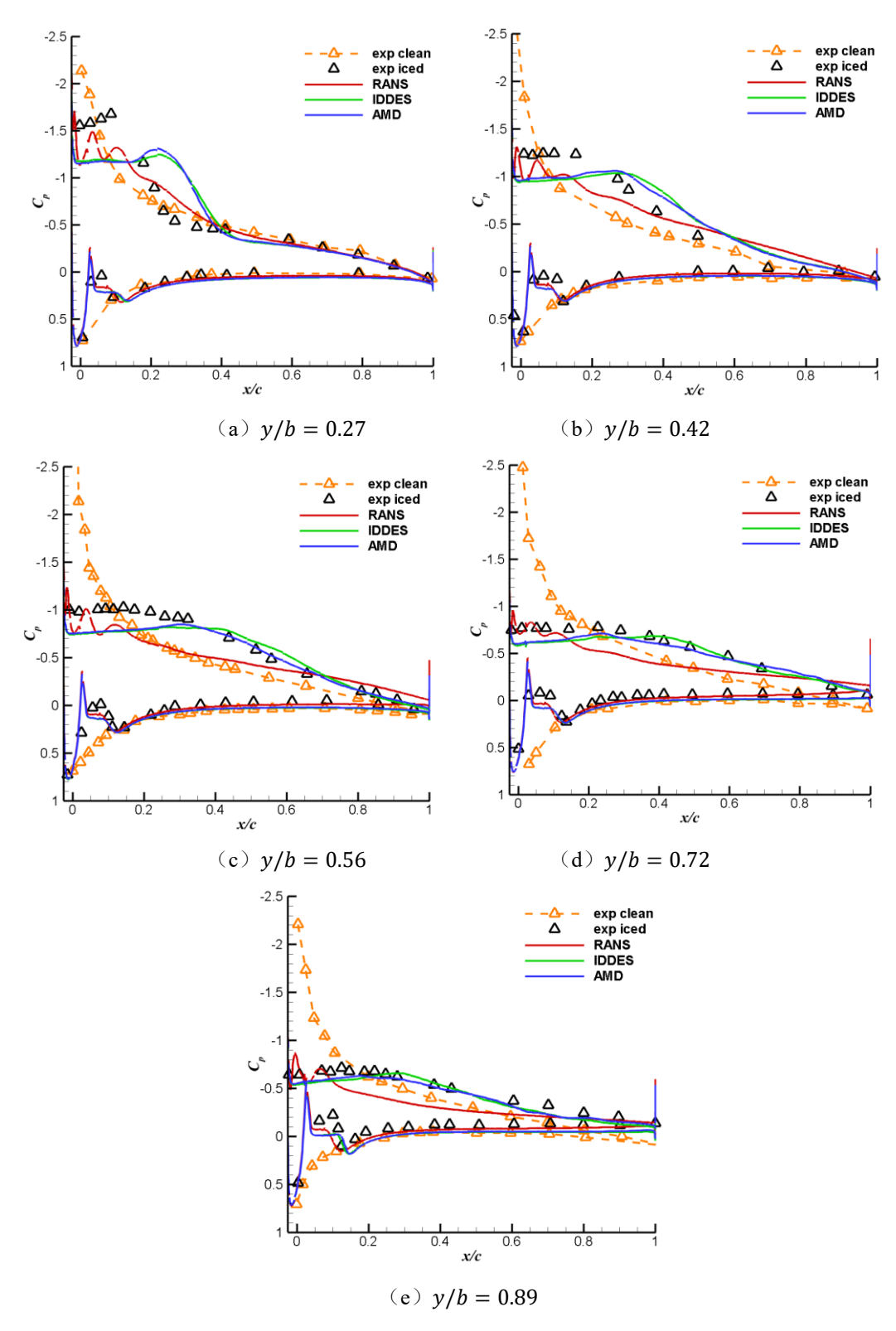


Figure 10: Mean pressure coefficient C_p distribution at different spanwise positions

Comparing the pressure coefficient distribution at different spanwise positions, it can be observed that as the spanwise position increases, the width of the pressure plateau gradually increases. This indicates that from the wing root to the wingtip, the vortex structures gradually grow, and there is noticeable spanwise flow. Comparing the results obtained from the standard IDDES and AMD-IDDES methods, it is also evident that the AMD-IDDES method provides a more accurate prediction of the pressure recovery region, while the IDDES method predicts a longer separation bubble.

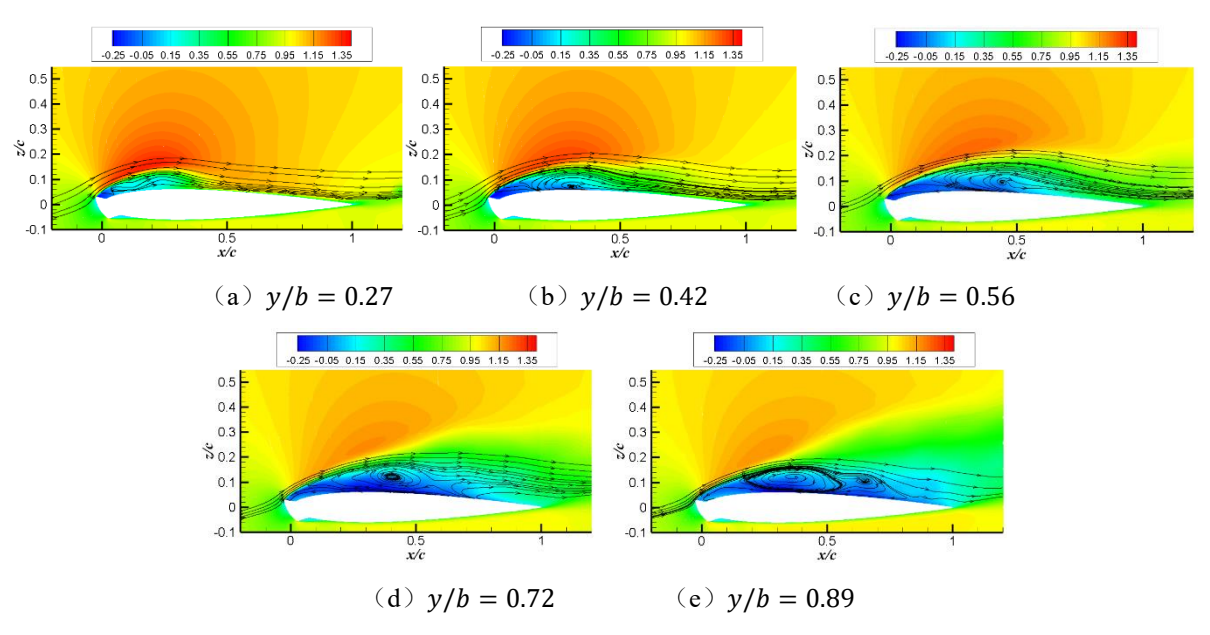


Figure 11: Mean streamwise velocity U_x/U_∞ and streamlines at different spanwise positions by IDDES

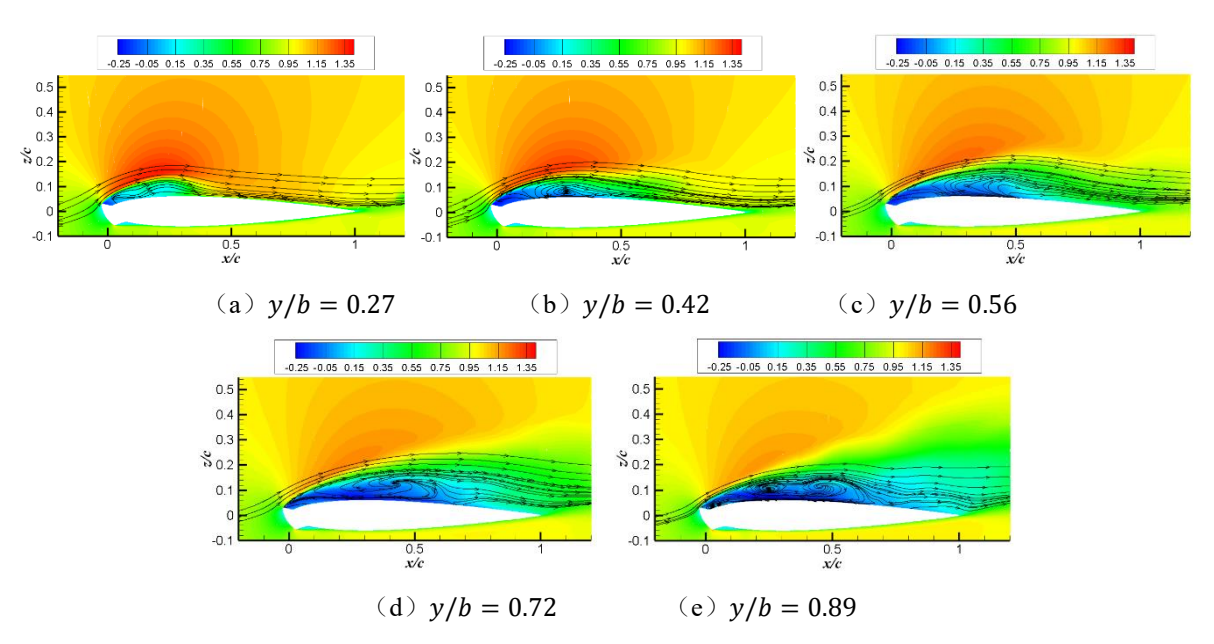


Figure 12: Mean streamwise velocity U_x/U_∞ and streamlines at different spanwise positions by AMD-IDDES

Figure 11 and Figure 12 show the mean streamwise velocity distribution at different spanwise positions, while Figure 13, Figure 14, and Figure 15 further present the mean streamwise velocity distribution at different chordwise positions (x/c = 0.01, 0.15, 0.30, 0.50). It can be observed that the flow distributions simulated by the AMD-IDDES and IDDES methods are generally similar, but the resulting vortex structures differ significantly. Near the wing root, the AMD-IDDES method, due to its smaller initial eddy viscosity, is able to resolve vortex structures earlier, whereas the IDDES

method, with its larger eddy viscosity, severely delays the K-H instability. Near the wingtip, the IDDES method, due to the delayed separation of the shear layer, results in larger downstream vortex structures. Deck and Thorigny [16] refer to these large-scale structures as "overly coherent" structures.

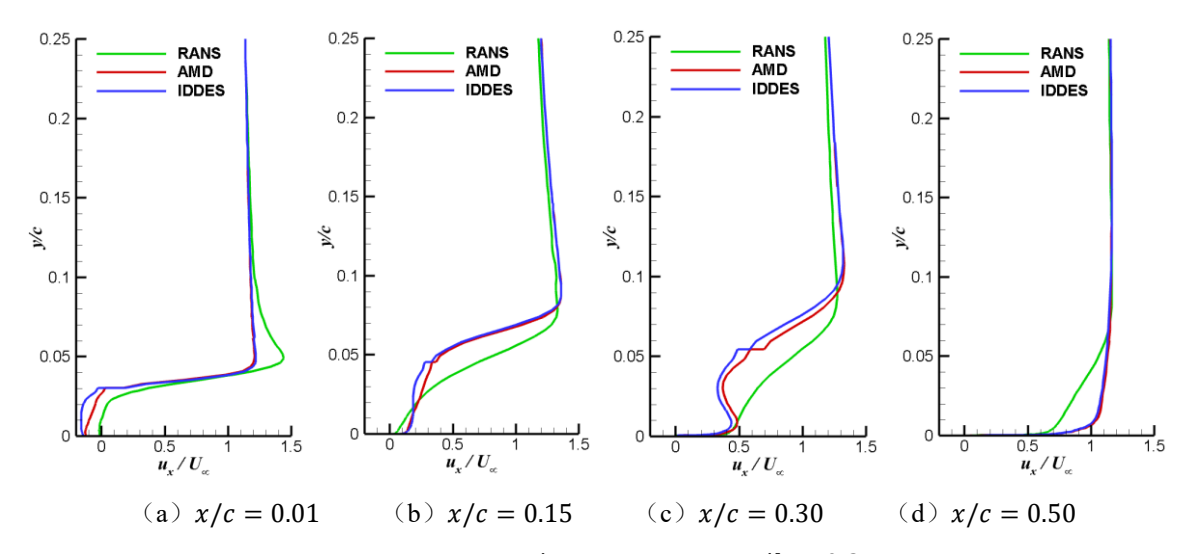


Figure 13: Mean streamwise velocity U_x/U_∞ distribution at z/b=0.27 for different methods

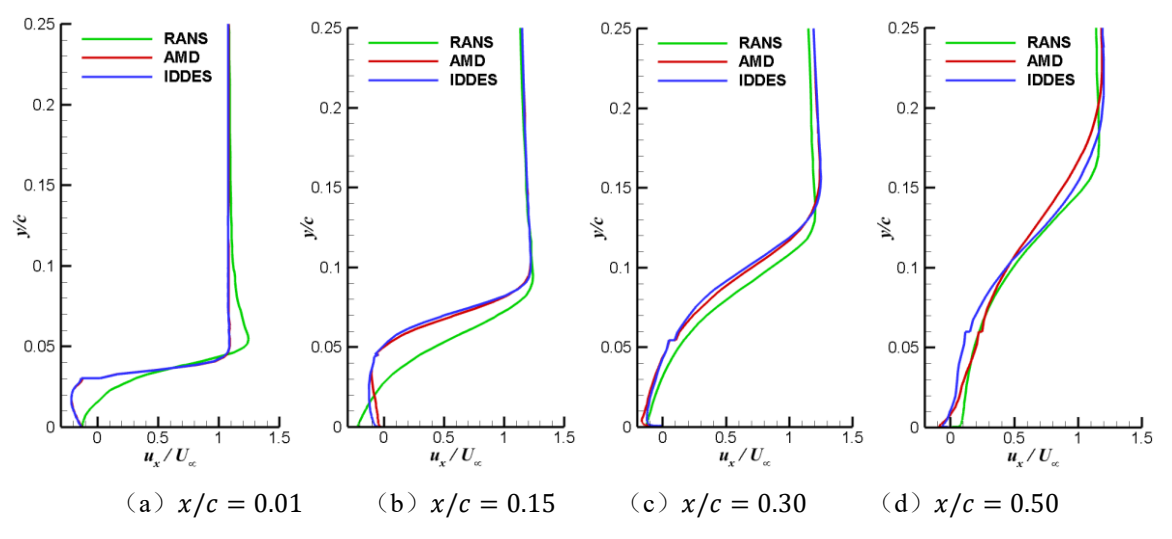


Figure 14: Mean streamwise velocity U_x/U_∞ distribution at z/b=0.56 for different methods

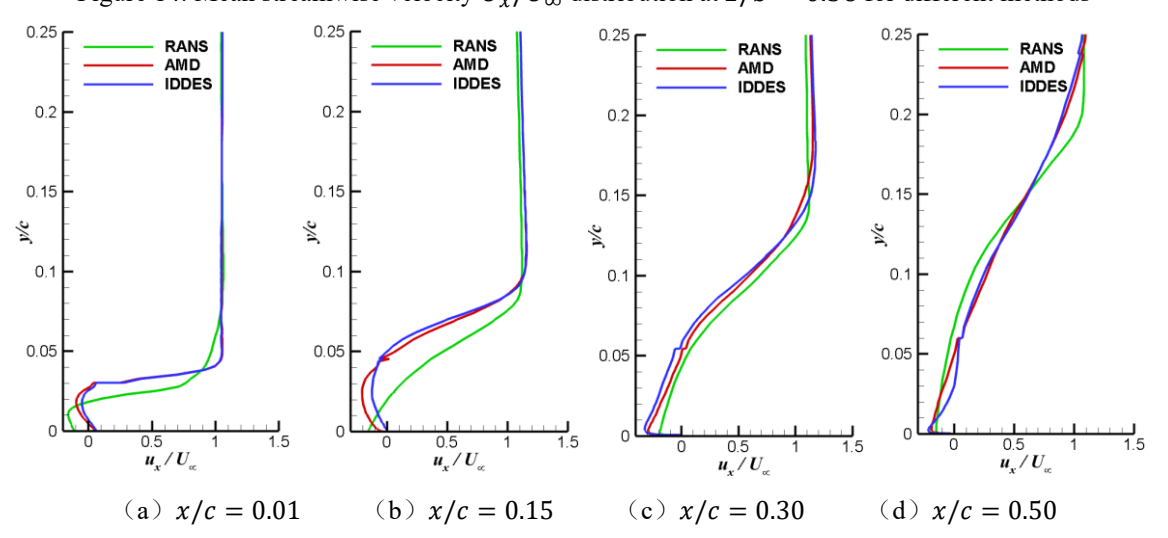


Figure 15: Mean streamwise velocity U_x/U_∞ distribution at z/b = 0.89 for different methods

5. Conclusion

In this study, the flow characteristics around a swept wing with ice accretion were investigated using both the standard IDDES method and the AMD-IDDES method. A detailed numerical analysis and comparison were conducted to reveal the effects of ice accretion on the aerodynamic performance of the wing and to assess the advantages of the AMD-IDDES method in improving simulation accuracy.

The comparison of instantaneous flow fields at different spanwise positions shows that the AMD-IDDES method effectively reduces the eddy viscosity in the shear layer separation region, enabling the earlier resolution of leading-edge vortex structures and mitigating the "gray area issue" commonly observed in the standard IDDES method. The AMD-IDDES method also demonstrated higher accuracy in predicting vorticity distribution within the shear layer and pressure recovery regions.

The pressure distribution results indicate that ice accretion at the leading edge replaces the leading-edge suction peak with an almost constant pressure plateau, which extends over approximately 20% to 40% of the chord length, suggesting the presence of a leading-edge separation bubble. In the pressure recovery region, the AMD-IDDES method provides a more accurate prediction of pressure distribution, whereas the standard IDDES method tends to overpredict the length of the separation bubble. Furthermore, the spanwise pressure distribution reveals that the width of the pressure plateau increases with increasing spanwise position, reflecting the growth of flow structures and the presence of significant spanwise flow.

The velocity distribution results further reveal differences in the flow structures predicted by the two methods. Near the wing root, the AMD-IDDES method, due to its lower initial eddy viscosity, can resolve the initial vortex structures earlier, whereas the standard IDDES method exhibits excessive eddy viscosity, which severely delays the development of Kelvin–Helmholtz (K-H) instability. Near the wingtip, the standard IDDES method delays shear layer separation, resulting in larger downstream vortex structures, which Deck and Thorigny referred to as "overly coherent" structures. In summary, the AMD-IDDES method demonstrates higher accuracy in simulating the complex flow characteristics of swept wings with ice accretion, particularly in shear layer separation, pressure recovery, and leading-edge vortex resolution. This study provides valuable insights for further improving the prediction methods for iced airfoil aerodynamic performance and enhancing the applicability of turbulence models.

Acknowledgments

This work was supported by the National Natural Science Foundation of China (Grant Nos. 12388101, 12372288, U23A2069, and 92152301) and the Jilin Province Science and Technology Development Program, China Grant No. 20220301013GX. The authors would like to express their gratitude to Jiawei Chen and Shaoguang Zhang for their insightful discussions.

References

- [1] Bragg, M. B., Broeren, A. P., and Stirling, L., "Iced-Airfoil and Wing Aerodynamics," *SAE Technical Papers*, 2003. https://doi.org/10.4271/2003-01-2098
- [2] Bragg, M., Broeren, A., and Stirling, L., "Ice-Airfoil Aerodynamics," *Progress in Aerospace Sciences PROG AEROSP SCI*, Vol. 41, 2005, pp. 323–362. https://doi.org/10.1016/j.paerosci.2005.07.001
- [3] Xiao, M., "Numerical Study of the Unsteady Separated Flow around Iced Airfoils," Master's Thesis. Tsinghua University, 2019.
- [4] Ratvasky, T. P., Barnhart, B. P., and Lee, S., "Current Methods Modeling and Simulating Icing Effects on Aircraft Performance, Stability, Control," *Journal of Aircraft*, Vol. 47, No. 1, 2010, pp. 201–211. https://doi.org/10.2514/1.44650
- [5] Menter, F., "Zonal Two Equation K-w Turbulence Models For Aerodynamic Flows," presented at the 23rd Fluid Dynamics, Plasmadynamics, and Lasers Conference, Orlando,FL,U.S.A., 1993. https://doi.org/10.2514/6.1993-2906
- [6] Shur, M., Spalart, P., Strelets, M., and Travin, A., "A Hybrid RANS-LES Approach with Delayed-DES and Wall-Modelled LES Capabilities," *International Journal of Heat and Fluid Flow*, Vol. 29, 2008, pp. 1638–1649. https://doi.org/10.1016/j.ijheatfluidflow.2008.07.001
- [7] Gritskevich, M., Garbaruk, A., Schütze, J., and Menter, F., "Development of DDES and IDDES Formulations for the K-ω Shear Stress Transport Model," *Flow, Turbulence and Combustion*, Vol. 88, 2012. https://doi.org/10.1007/s10494-011-9378-4

- [8] Rozema, W., Bae, H. J., Moin, P., and Verstappen, R., "Minimum-Dissipation Models for Large-Eddy Simulation," *Physics of Fluids*, Vol. 27, 2015. https://doi.org/10.1063/1.4928700
- [9] Haering, S. W., Lee, M., and Moser, R. D., "Resolution-Induced Anisotropy in Large-Eddy Simulations," *Physical Review Fluids*, Vol. 4, No. 11, 2019, p. 114605. https://doi.org/10.1103/PhysRevFluids.4.114605
- [10] Zhou, Z., Xiao, M., Li, D., and Zhang, Y., "Enhanced Delayed Detached-Eddy Simulation with Anisotropic Minimum Dissipation Subgrid Length Scale," *Physics of Fluids*, Vol. 37, No. 2, 2025, p. 025152. https://doi.org/10.1063/5.0246596
- [11] Xiao, M., and Zhang, Y., "Improved Prediction of Flow Around Airfoil Accreted with Horn or Ridge Ice," *AIAA Journal*, Vol. 59, No. 6, 2021, pp. 2318–2327. https://doi.org/10.2514/1.J059744
- [12] Diebold, J. M., Broeren, A. P., and Bragg, M., "Aerodynamic Classification of Swept-Wing Ice Accretion," presented at the 5th AIAA Atmospheric and Space Environments Conference, San Diego, CA, 2013. https://doi.org/10.2514/6.2013-2825
- [13] Bragg, M., Khodadoust, A., Soltani, R., Wells, S., and Kerho, M., "Aerodynamic Measurements on a Finite Wing with Simulated Ice," presented at the 9th Applied Aerodynamics Conference, Baltimore, MD, U.S.A., 1991. https://doi.org/10.2514/6.1991-3217
- [14] Bragg, M., Khodadoust, A., Soltani, R., Wells, S., and Kerho, M., "Effect of a Simulated Ice Accretion on the Aerodynamics of a Swept Wing," presented at the 29th Aerospace Sciences Meeting, Reno,NV,U.S.A., 1991. https://doi.org/10.2514/6.1991-442
- [15] Lee, D., Kawai, S., Nonomura, T., Anyoji, M., Aono, H., Oyama, A., Asai, K., and Fujii, K., "Mechanisms of Surface Pressure Distribution within a Laminar Separation Bubble at Different Reynolds Numbers," *Physics of Fluids*, Vol. 27, 2015. https://doi.org/10.1063/1.4913500
- [16] Deck, S., and Thorigny, P., "Unsteadiness of an Axisymmetric Separating-Reattaching Flow: Numerical Investigation," *Physics of Fluids*, Vol. 19, No. 6, 2007, p. 065103. https://doi.org/10.1063/1.2734996